Monthly Notices
of the
ROYAL ASTRONOMICAL SOCIETY

MNRAS **429,** 3230–3237 (2013) doi:10.1093/mnras/sts585

Inferring the mass of submillimetre galaxies by exploiting their gravitational magnification of background galaxies

H. Hildebrandt,[1,2⋆] L. van Waerbeke,[1] D. Scott,[1] M. Béthermin,[3,4] J. Bock,[5,6] D. Clements,[7] A. Conley,[8] A. Cooray,[5,9] J. S. Dunlop,[10] S. Eales,[11] T. Erben,[2] D. Farrah,[12] A. Franceschini,[13] J. Glenn,[8,14] M. Halpern,[1] S. Heinis,[15] R. J. Ivison,[16,17] G. Marsden,[1] S. J. Oliver,[18] M. J. Page,[19] I. Pérez-Fournon,[20,21] A. J. Smith,[18] M. Rowan-Robinson,[7] I. Valtchanov,[22] R. F. J. van der Burg,[23] J. D. Vieira,[5] M. Viero[5] and L. Wang[18]

[1]*Department of Physics and Astronomy, University of British Columbia, 6224 Agricultural Road, Vancouver, BC V6T 1Z1, Canada*
[2]*Argelander-Institut für Astronomie, Auf dem Hügel 71, D-53121 Bonn, Germany*
[3]*Laboratoire AIM-Paris-Saclay, CEA/DSM/Irfu – CNRS – Université Paris Diderot, CE-Saclay, pt courrier 131, F-91191 Gif-sur-Yvette, France*
[4]*Institut d'Astrophysique Spatiale (IAS), bâtiment 121, Université Paris-Sud 11 and CNRS (UMR 8617), F-91405 Orsay, France*
[5]*California Institute of Technology, 1200 East California Boulevard, Pasadena, CA 91125, USA*
[6]*Jet Propulsion Laboratory, 4800 Oak Grove Drive, Pasadena, CA 91109, USA*
[7]*Astrophysics Group, Imperial College London, Blackett Laboratory, Prince Consort Road, London SW7 2AZ*
[8]*Department of Astrophysical and Planetary Sciences, CASA 389-UCB, University of Colorado, Boulder, CO 80309, USA*
[9]*Department of Physics and Astronomy, University of California, Irvine, CA 92697, USA*
[10]*SUPA, Institute for Astronomy, University of Edinburgh, Royal Observatory, Edinburgh EH9 3HJ*
[11]*Cardiff School of Physics and Astronomy, Cardiff University, Queens Buildings, The Parade, Cardiff CF24 3AA*
[12]*Department of Physics, Virginia Tech, Blacksburg, VA 24061, USA*
[13]*Dipartimento di Astronomia, Università di Padova, Vicolo Osservatorio 3, I-35122 Padova, Italy*
[14]*Center for Astrophysics and Space Astronomy, University of Colorado, Boulder, 389 UCB, CO, USA*
[15]*Department of Physics and Astronomy, The Johns Hopkins University, 3400 North Charles Street, Baltimore, MD 21218, USA*
[16]*Institute for Astronomy, University of Edinburgh, Royal Observatory, Blackford Hill, Edinburgh EH9 3HJ*
[17]*UK Astronomy Technology Centre, Royal Observatory, Blackford Hill, Edinburgh EH9 3HJ*
[18]*Astronomy Centre, Department of Physics and Astronomy, University of Sussex, Brighton BN1 9QH*
[19]*Mullard Space Science Laboratory, University College London, Holmbury St Mary, Dorking, Surrey RH5 6NT*
[20]*Instituto de Astrofísica de Canarias (IAC), E-38200 La Laguna, Tenerife, Spain*
[21]*Departamento de Astrofísica, Universidad de La Laguna (ULL), E-38206 La Laguna, Tenerife, Spain*
[22]*European Space Astronomy Centre, Herschel Science Centre, ESA, E-28691 Villanueva de la Cañada, Spain*
[23]*Leiden Observatory, Leiden University, Niels Bohrweg 2, NL-2333 CA Leiden, the Netherlands*

Accepted 2012 December 6. Received 2012 November 26; in original form 2012 November 11

ABSTRACT

Dust emission at submillimetre wavelengths allows us to trace the early phases of star formation in the Universe. In order to understand the physical processes involved in this mode of star formation, it is essential to gain knowledge about the dark matter structures – most importantly their masses – that submillimetre galaxies live in. Here we use the magnification effect of gravitational lensing to determine the average mass and dust content of submillimetre galaxies with 250 μm flux densities of $S_{250} > 15$ mJy selected using data from the Herschel Multi-tiered Extragalactic Survey. The positions of hundreds of submillimetre foreground lenses are cross-correlated with the positions of background Lyman-break galaxies at $z \sim 3$–5 selected using optical data from the Canada–France–Hawaii Telescope Legacy Survey. We detect a cross-correlation signal at the 7σ level over a sky area of 1 deg^2, with ∼80 per cent of this signal being due to magnification, whereas the remaining ∼20 per cent comes from dust extinction. Adopting some simple assumptions for the dark matter and dust profiles and the redshift

⋆ E-mail: hendrikhildebrandt@gmail.com

distribution enables us to estimate the average mass of the haloes hosting the submillimetre galaxies to be $\log_{10}[M_{200}/\mathrm{M}_{\odot}] = 13.17^{+0.05}_{-0.08}$(stat.) and their average dust mass fraction (at radii of >10 kpc) to be $M_{\rm dust}/M_{200} \approx 6 \times 10^{-5}$. This supports the picture that submillimetre galaxies are dusty, forming stars at a high rate, reside in massive group-sized haloes and are a crucial phase in the assembly and evolution of structure in the Universe.

Key words: gravitational lensing: weak – galaxies: high-redshift – submillimetre: galaxies.

1 INTRODUCTION

In the current picture galaxies form in the centres of the gravitational potential wells of dark matter haloes, when gas cools and star formation sets in (Eggen, Lynden-Bell & Sandage 1962). However, many of the observed properties of galaxies – e.g. scaling laws between different observables like the Faber & Jackson (1976) relation, the Tully & Fisher (1977) relation and the m–σ relation (Ferrarese & Merritt 2000) – remain to be explained by a complete theory of galaxy formation and evolution. We know from observations in the $z < 1$ Universe that star formation efficiency, i.e. the fraction of baryonic mass turned into stars, depends on the environment, most importantly on the mass of the dark matter halo as shown by Leauthaud et al. (2012). The bulk of star formation, however, happened at earlier cosmic epochs (Madau et al. 1996), when the Universe was less than half of its current age, which necessitates studies at high redshift ($z \gtrsim 1$).

Young stars are still enveloped in clouds of gas and dust, and therefore most of their radiation is absorbed by dust, and re-emitted at far-infrared wavelengths. Since this is the dominant source of emission at these wavelengths, the luminosity of a galaxy in the far-infrared wavelength range is directly related to the amount of young stars, and therefore the rate of star formation. Submillimetre telescopes are sensitive to this radiation. Moreover, the detection of this light is less sensitive to redshift than in the optical, due to the fortunate shape of the spectral energy distributions of galaxies in the submillimetre regime yielding samples of star-forming galaxies over a wide redshift range. Establishing a picture of the dark matter environment of these submillimetre galaxies through measuring their total (i.e. baryonic plus dark matter) masses is hence a fundamental ingredient for understanding the build-up of stellar mass over cosmic time.

Gravitational lensing is the most direct method of measuring mass in the distant Universe, irrespective of whether it consists of dark or baryonic matter, and independent of any assumptions about its dynamical state. Thus, it represents a powerful tool for measuring the masses of dark matter structures, both using fewer astrophysical assumptions and being complementary to, e.g. velocity dispersion measurements. In many cases the lensing effect of an individual deflector is too weak to be detected. In weak gravitational lensing (WL; see e.g. Bartelmann & Schneider 2001) a statistical approach is used, averaging the signals of many lenses and/or sources.

In order to detect the effects of WL by a lens population, a suitable source population is needed that lies behind the lenses (from the observer's point of view). The extended redshift distribution of submillimetre galaxies means that most potential background galaxies are spatially unresolved in even the best ground-based optical data. Hence the traditional shear technique of WL, which requires ellipticity estimates, cannot be used in this particular case, and one has to turn to the magnification technique, which does not require resolved sources (van Waerbeke et al. 2010).

Here we measure the WL magnification effect of a submillimetre galaxy sample to estimate their average dark matter halo density profiles. As background sources we use optically selected Lyman-break galaxies (LBGs; Steidel et al. 1996) which are located at even higher redshifts. The submillimetre as well as the optical data is described in Section 2. An outline of the magnification technique is given in Section 3. Results are presented in Section 5 and discussed in Section 6. A summary and an outlook are given in Section 7. We assume a *Wilkinson Microwave Anisotropy Probe* 7-year (*WMAP*7) cosmology throughout (Komatsu et al. 2011): $(\Omega_{\rm M}, \Omega_{\Lambda}, h, \sigma_8) = (0.27, 0.73, 0.70, 0.81)$.

2 DATA

2.1 Submillimetre data

The submillimetre galaxies are selected from the Herschel Multi-tiered Extragalactic Survey (HerMES; Oliver et al. 2010; HerMES Collaboration et al. 2012), observed with the Spectral and Photometric Imaging Receiver (SPIRE; Griffin et al. 2010) on board the *Herschel Space Observatory* in the Cosmic Evolution Survey (COSMOS; Scoville et al. 2007) field. The catalogue[1] was constructed by the HerMES team, using blind extraction at 250 μm and a prior-based extraction for the other two wave bands at 350 and 500 μm. Details can be found in Roseboom et al. (2010). Note that these submillimetre galaxies constitute the lenses here and not the sources as in Wang et al. (2011).

Unlike 'classical' submillimetre sources detected at longer wavelength like, e.g. SCUBA-type (Holland et al. 1999) galaxies, the galaxies detected by SPIRE at 250 μm do not show a strong negative k-correction (Franceschini et al. 1991; Blain & Longair 1993). Hence their redshift distribution does not extend to as high redshifts, which is beneficial for the magnification measurement presented here, since it allows for easier separation between the submillimetre lenses and the LBG sources in redshift.

The beam size of *Herschel* at 250 μm is full width at half-maximum (FWHM) ≈ 18 arcsec. The centroids of the submillimetre galaxies in each sky coordinate are known to $\Delta\alpha = \Delta\delta = 0.6\,\mathrm{FWHM/SNR}$, where SNR is the signal-to-noise ratio of the detection (Ivison et al. 2007). The mean SNR of our lenses is $\overline{\mathrm{SNR}} = 5.3$, which corresponds to centroid errors of $\Delta\alpha = \Delta\delta = 2.0$ arcsec. Additionally, the pointing accuracy of *Herschel* is limited to $\approx$2 arcsec as well (Pilbratt et al. 2010). We add these two contributions to the centroid error in quadrature and account for this angular uncertainty in the modelling (see Section 4).

2.2 Optical data

The central part of the COSMOS field (1 deg^2) was targeted with the MegaCam imager on the Canada–France–Hawaii Telescope (CFHT) as part of the CFHT Legacy Survey. Very deep images (5σ limiting magnitudes for point sources of 26.5–28.0) in the *ugriz*

[1] Available at the HeDaM on-line data base: http://hedam.oamp.fr/HerMES/

bands from the CARS project (Erben et al. 2009; Hildebrandt et al. 2009a) were used to select a sample of ∼17 500 LBGs (Hildebrandt et al. 2009a; Hildebrandt, van Waerbeke & Erben 2009b) at redshifts $z \sim 3$–5. These are too distant to be resolved in the optical data, but they constitute an ideal sample for magnification measurements.

This set of LBGs has been studied in detail in the literature. Their clustering properties are described in Hildebrandt et al. (2009a) and a measurement of the LBG luminosity function based on this data set is presented in van der Burg, Hildebrandt & Erben (2010). Furthermore, these LBGs were already used as background sources for a magnification measurement in a previous study (Hildebrandt et al. 2009b), but then using normal galaxies selected by photometric redshifts as lenses.

2.3 Redshift distributions

The HerMES catalogue contains 3402 objects in the common area of the optical and submillimetre data. For the mass measurement we only consider lenses with a submillimetre flux density at 250 μm of $S_{250} > 15$ mJy. This is necessary because confusion (and other effects) is more severe at fainter flux densities in the *Herschel* data, which would make the estimation of a redshift distribution for the lenses very problematic. This redshift distribution is needed to interpret the signal, since it depends on the lens-source geometry, and to estimate a mass. We further apply a colour cut on the submillimetre lenses to enhance the separation in redshift. We require the ratio of the flux densities at 500 and 250 μm to be $S_{500}/S_{250} < 0.5$. This leaves us with 587 lenses. The measured and simulated redshift distributions of the lenses are presented in Béthermin et al. (2011, 2012b). We use the simulated one in the following. The model of the redshift distribution of the sources is taken from Hildebrandt et al. (2009a). These distributions are plotted in Fig. 1, showing only marginal overlap.

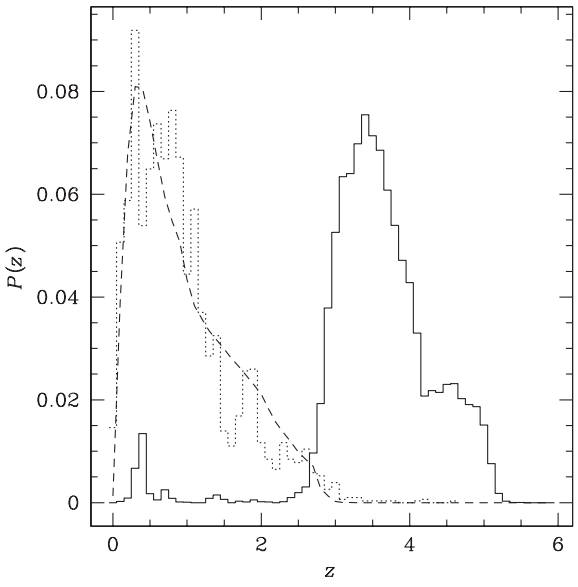

Figure 1. Redshift distributions of the submillimetre lenses (dashed: simulation; dotted: photometric redshifts) and the LBG sources (solid) used in the magnification measurement. The separation in redshift is not perfect and therefore we model the contribution from physical clustering (due to redshift overlap) to the cross-correlation signal.

3 TECHNIQUE

The measurement described here is technically similar to the previous measurement by Wang et al. (2011) using submillimetre galaxies and magnification, but conceptually it is very different because here we are studying the effects of lensing *by* submillimetre galaxies rather than the effects of lensing by other sources *on* submillimetre galaxies (see also Blake et al. 2006, for a related cross-correlation measurement). Thus, we can study how their dark matter haloes deflect light and estimate their average mass through this effect, which was not possible when the submillimetre galaxies were used as sources.

As detailed in other studies (van Waerbeke et al. 2010; Hildebrandt et al. 2011) magnification is a particularly useful tool for measuring the average masses of objects at high redshifts because – unlike shear-based weak lensing methods – it does not require the background sources to be resolved. A large fraction of the submillimetre galaxies studied here have redshifts $z > 1$. With the best optical ground-based data there are very few objects at such high redshifts that could be resolved and used as background sources for shear measurements because of the seeing-limited size of the optical point spread function (PSF). Even with optical imaging data from the *Hubble Space Telescope* it becomes increasingly difficult to resolve objects with $z \gtrsim 1.5$ due to PSF size. Thus, the population of submillimetre galaxies studied here represents an ideal lens sample for magnification when LBGs are used as background sources.

The WL magnification effect of the lenses increases the fluxes of background objects and shifts their positions on the sky. This induces a change in their number density, which leads to angular correlations in the positions of lenses and sources on the sky, even in the absence of physical clustering, i.e. when both populations are well separated in redshift (Scranton et al. 2005; Hildebrandt et al. 2009b). Depending on the slope of the magnitude number counts of the source sample, $\alpha = 2.5\,\mathrm{d}\log[N(m)]/\mathrm{d}m$, a positive or a negative cross-correlation is expected from WL theory. Bright galaxies with typically steep slopes ($\alpha - 1 > 0$) should show positive correlations, and faint galaxies, with shallow slopes ($\alpha - 1 < 0$), should show anticorrelations.

WL magnification is not the only effect that can cross-correlate the sky position of objects that are far apart along the line of sight. Extinction by dust in the foreground objects can also lead to a characteristic depletion of the number density of background objects, and this has to be included in the modelling to correctly interpret the cross-correlation signal. This behaviour can be described by an effective slope α_{eff} as detailed below.

For this kind of measurement it is particularly important to minimize the overlap in redshift between the lens and source populations to suppress a systematic bias due to physical cross-correlations, which can be much larger than the magnification/extinction signal.

The cross-correlation functions are estimated using the estimator from Landy & Szalay (1993) based on pair counts:

$$w(\theta) = \frac{\mathrm{D_1D_2} - \mathrm{D_1R} - \mathrm{D_2R}}{\mathrm{RR}} + 1, \quad (1)$$

with $\mathrm{D_1D_2}$ being the number of submillimetre–LBG pairs in the angular range $[\theta, \theta + \delta\theta]$ normalized by the product of their total numbers, $\mathrm{D}_i\mathrm{R}$ being the normalized number of pairs between the submillimetre/LBG catalogue and a random catalogue (with the same surface geometry) in that angular range and RR being the normalized number of pairs in the random catalogue in that angular range. By choosing a random catalogue that is much larger

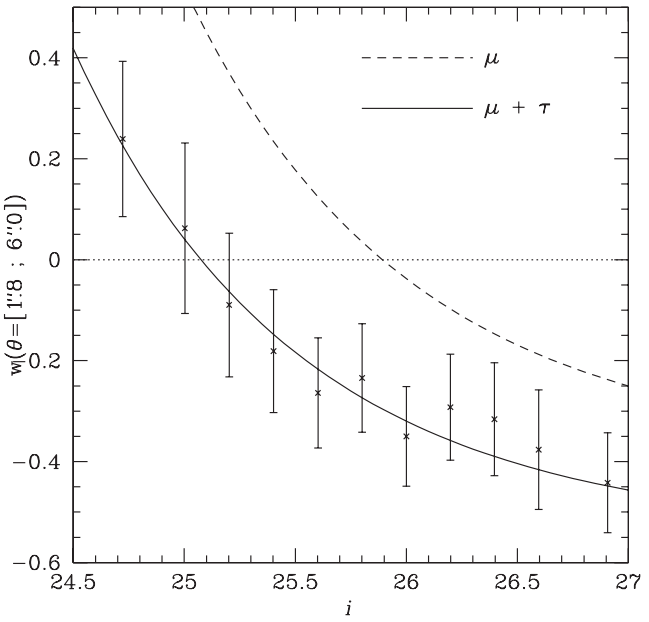

Figure 2. Amplitude of the angular cross-correlation function between 3402 submillimetre lenses and LBG sources as a function of the LBG i-band magnitude in the angular interval $1.8 < \theta < 6.0$ arcsec. Errors are Poissonian. The dashed line represents the expected amplitude if there was only magnification. The solid line represents a more realistic model including the effects of extinction by dust in the lenses.

than the data catalogues the shot noise introduced by the random catalogue is suppressed.

It has been shown in Ménard et al. (2003) and Scranton et al. (2005) that the signal-to-noise ratio of a magnification measurement can be boosted when every background galaxy is given a weight that corresponds to the $\alpha - 1$ value at its magnitude. The same can be done if there is additional dust extinction by instead using an effective weight, $\alpha_{\rm eff} - 1$.

For the optimally weighted correlation function the same estimator is used, but D_1D_2 and D_2R are replaced by the sums of weights instead of the number of pairs (Hildebrandt et al. 2009b). The weights are $\alpha_{\rm eff} - 1$ (see Section 5 for a definition) for the LBG in each pair accounting for the fact that part of the signal is due to extinction. Such a weighting maximizes the signal-to-noise ratio of the magnification/extinction measurement (Ménard et al. 2003; Scranton et al. 2005). The gain is considerable for cases where the weight changes appreciably over the whole range of magnitudes of the background sample (typically for very deep data as used here; see also Fig. 2).

4 THEORETICAL BACKGROUND

We assume that the haloes hosting the submillimetre galaxies can be described by a single NFW (Navarro, Frenk & White 1996) halo. This model has two parameters, the mass M_{200} and the concentration c. Detailed dark matter N-body simulations show that these two parameters are strongly correlated and a relation can be established between the two. Here, we use the relation by Prada et al. (2012) to reduce the number of parameters in our mass model. The magnification profile of an NFW halo is described in Wright & Brainerd (2000).

We model the signal of the optimally weighted cross-correlation function in the following way:

$$w_{\rm opt}(\theta) = w_\mu(\theta) + w_\tau(\theta) + w_{\rm cc}(\theta), \quad (2)$$

where w_μ describes the contribution from magnification, w_τ describes the contribution from dust extinction in the lens galaxies and $w_{\rm cc}$ is the physical clustering part of the signal that is due to redshift overlap between lenses and sources and should be minimized.

The magnification signal can be calculated from lensing theory:

$$w_\mu(\theta) = \int_{m_{\rm min}}^{m_{\rm max}} [\alpha_{\rm eff}(m) - 1] \left[\mu(\theta)^{\alpha(m)-1} - 1\right] \hat{N}(m)\,{\rm d}m, \quad (3)$$

with $m_{\rm min/max}$ being the faintest and brightest magnitudes of the background sample, $\alpha_{\rm eff}(m) - 1$ being the effective weight, $\mu(\theta)$ being the magnification profile of an NFW halo,[2] $\alpha(m) - 1 = 2.5\,{\rm dlog}\,[N(m)]/{\rm d}m - 1$ being the weight in absence of extinction (taken from the LBG luminosity function of van der Burg et al. 2010) and $\hat{N}(m)$ being the normalized number counts of the LBGs.

The dust absorption A is related to the optical depth through

$$A = 2.5/\ln(10)\tau = 1.08\tau. \quad (4)$$

We assume that A and the magnification excess $\delta\mu = \mu - 1$ are related by[3]

$$A = c_{\rm d}\delta\mu. \quad (5)$$

Here we assume that this is true on average. The redshift dependence of the dust extinction and the magnification is certainly different. Hence haloes at different redshift will contribute differently to the magnification and extinction signals. We neglect this effect in the following but note that firm conclusions on the shape of the dust profile can only be drawn if such effects are included in the modelling. The mass estimate is not directly affected by this simplification. Under these assumptions the dust signal becomes

$$w_\tau(\theta) = \int_{m_{\rm min}}^{m_{\rm max}} [\alpha_{\rm eff}(m) - 1] \times \left[1.08\, c_{\rm d} 10^{-0.4\alpha(m)}\, \delta\mu(\theta) - 1\right] \hat{N}(m)\,{\rm d}m. \quad (6)$$

The contribution from physical clustering to the angular correlation function is modelled by

$$w_{\rm cc}(\theta) = \int_{m_{\rm min}}^{m_{\rm max}} [\alpha_{\rm eff}(m) - 1]\, b_1 b_2 w_{\rm DM}(\theta) \hat{N}(m)\,{\rm d}m, \quad (7)$$

where $b_{1/2}$ are the average bias factors of the lenses and sources, respectively, and $w_{\rm DM}$ is the angular correlation function of the dark matter field.[4] We conservatively estimate $b_1 = b_2 = 2$ in our analysis.

5 RESULTS

The angular cross-correlation (unweighted) between the positions of all submillimetre lenses in the 1 deg^2 area (3402 objects; no flux

[2] For readability we do not include the redshift dependence here. But it should be clear that $\mu(\theta)$ has to be calculated by integrating over the redshift distributions of the lenses and sources.

[3] Note that this does not constrain the dust profile yet because $c_{\rm d}$ can be a function of angular scale.

[4] This is calculated with the equation from Limber (1953). We used the code by Hamana et al. (2004) for this. The contribution from physical clustering has to be weighed appropriately with the product of the redshift distributions of lenses and sources.

cut) and the LBG sources in different magnitude slices at close separations is shown in Fig. 2. Here we use one broad angular bin with $1.8 < \theta < 6.0$ arcsec. As expected, the positions of the brighter background galaxies are positively correlated with the positions of the lenses, while the positions of the fainter ones are anticorrelated. However, the dashed line, which shows the expected amplitude from magnification only, without dust extinction, does not fit the data points. The solid line represents the expected amplitude of the cross-correlation function assuming that on average the dust absorption is proportional to the magnification excess [note that this is well supported by results from Ménard et al. 2010, using Sloan Digital Sky Survey (SDSS) data]. We fit for the dust normalization constant $c_{\rm d}$, obtaining a best-fitting value of $c_{\rm d} = 0.35$. The overall normalization was left as another free parameter and both predictions were multiplied by this value. In both cases we model $N(m)$ from the LBG luminosity function estimates by van der Burg et al. (2010).

Ménard et al. (2010) found a value of $c_{\rm d} \approx 0.1$ using a magnitude-limited, optically selected, low-z galaxy sample from the SDSS. Thus, the submillimetre galaxies we study here are – not surprisingly – considerably more dusty (although the $c_{\rm d}$ values cannot be compared directly because of the different rest-frame wavelengths of the filters used for the selection of the lenses).

Physical clustering signals due to redshift overlap between lenses and sources are always positive. Thus, detecting a negative cross-correlation, as shown in Fig. 2, already suggests that we do not have significant redshift overlap here.

Here, we use all 3402 lenses detected in the submillimetre data to improve the statistics and be able to constrain the scaling between magnification and extinction. However, we limit the following analysis to the 587 objects with $S_{250} > 15$ mJy and $S_{500}/S_{250} < 0.5$, for which we can estimate a reliable redshift distribution (see Section 2.3). By applying the $c_{\rm d}$ value found from the whole sample of 3402 objects to the high-confidence sample of 587 objects we implicitly assume that the redshift distribution, as well as the scaling between $\delta\mu$ and A, does not differ significantly between the two samples. With the current data and models this cannot be tested directly and has to remain an assumption here.

In Fig. 3 the optimally weighted cross-correlation function between these 587 submillimetre galaxies and the full set of background LBGs is shown, with errors estimated from a jackknife resampling of the background sample. We detect a signal at the 7σ level. The best-fitting value for $c_{\rm d}$ (=0.35) that we take from the previous measurement indicates that the majority of this signal is due to magnification and not extinction. Note that the accurate relative contributions depend on the absolute value of the magnification itself (and hence also on angular scale). At small angular scales magnification contributes about 85 per cent to the signal, whereas at large angular scales its contribution drops to about 75 per cent.

We fit the model from equation (2) to the data, which represents the magnification of an NFW dark matter halo, as well as the extinction of a dust halo whose dust is distributed according to the same profile. Additionally we take the small contribution from physical cross-correlations $w_{\rm cc}$ into account, which is further suppressed because of the weighting scheme. Because of the fact that most of the background LBGs have negative weights, $\alpha_{\rm eff} - 1$, $w_{\rm cc}$ actually becomes negative in this optimally weighted case.[5] We also account for errors in the centroid positions of the submillimetre lenses due to the limited resolution of *Herschel*.

[5] This also means that not accounting for or underestimating $w_{\rm cc}$ would lead to an underestimate of the mass.

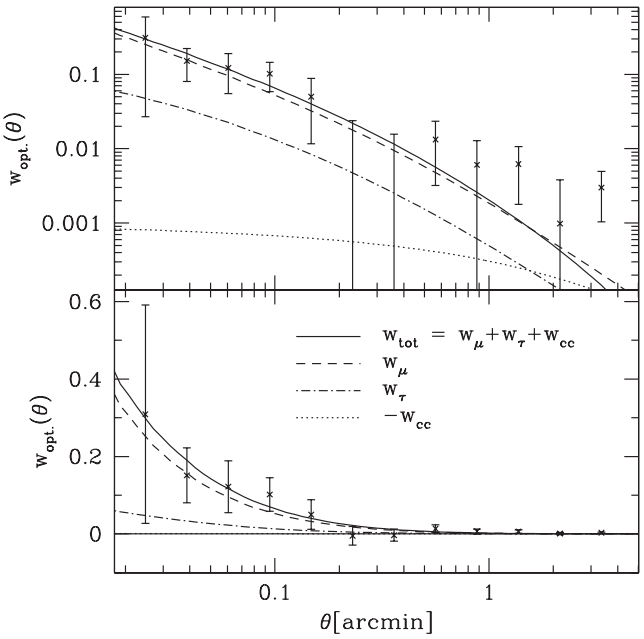

Figure 3. Optimally weighted angular correlation function between 587 submillimetre galaxies with 250 μm flux density $S_{250} > 15$ mJy and all background LBGs. The weights are based on the results presented in Fig. 2 with only the brightest LBGs getting a positive weight and the fainter ones all getting a negative weight. The solid line represents the best-fitting model, consisting of contributions from magnification (dashed line), dust extinction (dot–dashed) and a negative contribution from physical clustering between lenses and sources (dotted, and almost negligible). The top panel shows a logarithmic scale for the correlation amplitude whereas the bottom panel has a linear scale. Errors are estimated from a jackknife resampling of the background population.

The best-fitting estimate of the average NFW halo mass within r_{200} is $\log_{10}[M_{200}/{\rm M}_\odot] = 13.17^{+0.05}_{-0.08}$(stat.) or $M_{200} = 1.48^{+0.18}_{-0.25}$(stat.) $\times\, 10^{13}\,{\rm M}_\odot$, directly confirming that submillimetre galaxies are hosted by very massive haloes.

Note that by assuming that dust follows mass (see above) we can exploit the contribution from extinction to the signal in order to actually constrain the mass. The quoted error contains contributions from shot noise as well as from clustering of the background population. No uncertainties originating from the measurement of $c_{\rm d}$, the assumption that dust follows mass, the assumed redshift distributions or the physical clustering model are included here, because these uncertainties are very hard to quantify at the current stage, but could well be substantial.

Our best-fitting model also suggests that submillimetre galaxies are very dusty. Assuming that the extinction law of the dust in these galaxies is similar to that found in the Small Magellanic Cloud (Ménard et al. 2010), the dust mass fraction at the scales we are probing ($\gtrsim$10 kpc) can be estimated to be roughly $M_{\rm dust}/M_{200} \approx 6 \times 10^{-5}$.

6 DISCUSSION

6.1 Details of the modelling

The magnification exceeds $\mu = 1.5$ for the smallest scales that we are probing here, taking into account that the dust extinction

contributes 15 per cent of this signal. Thus, this is not strictly weak lensing but rather an intermediate regime between strong and weak lensing where a statistical technique – similar to what is used in weak lensing – is applied. Note that because of this we do not assume the weak lensing limit (i.e. $\delta\mu \ll 1$) in any part of the modelling.

Both, the magnification as well as the extinction, lead to a net depletion of background sources behind the submillimetre lenses, hence the negative average weight. Even without directly using colour information, we can still disentangle the two effects because we have a measurement of the average intrinsic luminosity function of the LBGs (van der Burg et al. 2010). Attributing the amplitude of the correlation function solely to either magnification or extinction would lead to inconsistencies as it is shown in Fig. 2.

6.2 Relation to clustering

Clustering measurements have been used to constrain the dark matter halo masses of submillimetre galaxies by interpreting their autocorrelation function in the framework of the halo model (Farrah et al. 2006; Cooray et al. 2010; Amblard et al. 2011; Hickox et al. 2012; Viero et al. 2012). While we also measure a correlation function here, the origin of the signal is very different. The lensing magnification method described here differs in some important aspects from such clustering measurements.

We actually try to suppress the physical clustering contribution to the cross-correlation function as much as possible by separating the submillimetre lenses and LBG sources in redshift. The autocorrelation signal that is used by physical clustering measurements represents a systematic nuisance in magnification studies. We model its small contribution to the cross-correlation function here and account for it in the mass measurement, but it is important to note that it is not used to estimate the mass.

In order to interpret an autocorrelation signal from physical clustering, some model for the galaxy bias has to be assumed. No such model is needed to interpret our lensing correlation function on small scales, under the assumption that all submillimetre galaxies are central galaxies to their haloes.

Another important difference between physical clustering measurements and lensing magnification is the different sensitivity to the shape of the redshift distribution. While the interpretation of the physical angular cross-correlation function depends critically on the width of the redshift distribution, lensing is fairly insensitive to this width because the lensing efficiency is a slowly changing function of redshift. It is mainly the mean redshift that is important here. However, this is only true as long as there is no redshift overlap between lenses and sources. Once there are physical cross-correlations contributing to the signal, as in the measurement presented here, the width becomes important again for estimating this contribution.

6.3 Comparison to abundance matching

We also roughly estimate the mass of haloes hosting the submillimetre galaxies from abundance matching (Béthermin, Doré & Lagache 2012a) using the following method. We compute the infrared luminosity of a source having the mean redshift and the mean flux of the *Herschel* sample. We convert this luminosity into star formation rate (SFR) using the Kennicutt (1998) constant ($1 \times 10^{-10}\,\mathrm{M_\odot\,yr^{-1}\,L_\odot^{-1}}$). We finally use the abundance matching results at this SFR and this mean redshift, using an interpolation between the two closest redshifts where the abundance matching was performed. This yields a mass estimate of $\log_{10}[M_{200}/\mathrm{M_\odot}] = 13.2 \pm 0.2$, in very good agreement with our magnification/extinction measurement.[6]

6.4 Notes on the submillimetre catalogue

This submillimetre galaxy lens sample represents a fairly faint population. Thus, the number of lenses that are lensed themselves is also very low. A completely negligible fraction of the signal shown in Fig. 3 is due to lensing of both, the lenses and the sources, by foreground structures in front of both (Heavens & Joachimi 2011).

When we use the full catalogue of 3402 objects for the determination of the constant c_d it is very probable that there are a large number of spurious objects in this sample. Note that this does not matter in that particular case because we are only interested in the relative amounts of magnification and extinction there. A spurious source should not add to either of the two and hence not change the result. For the actual mass measurement we use only galaxies with 250 μm flux densities of $S_{250} > 15$ mJy as lenses. Given the depth of the data this sample should not contain any spurious sources.

6.5 Limitations and possible extensions

There are several aspects that limit the accuracy of the measurement presented here. We have to use a redshift distribution based on a model for the submillimetre lenses to predict the magnification signal. Individual (photometric) redshifts for all submillimetre galaxies would certainly help to overcome any uncertainties in the modelling of their redshift distribution (Béthermin et al. 2012b).

The amount of physical cross-correlation, described by w_cc, depends on the redshift distribution of the LBGs, which is taken from simulations (Hildebrandt et al. 2009a). It should be noted that the choice here is actually quite pessimistic. With different plausible choices presented in Hildebrandt et al. (2009a), which are based on modified simulations, the overlap and hence amplitude of w_cc would decrease even further. The mass estimate is virtually unaffected by this very small change. We would like to stress that the optimal weighting of the correlation function greatly suppresses the physical cross-correlation. In order to boost the signal-to-noise ratio of the desired signal components each background galaxy is weighted with its expected responsiveness to the combined effects of magnification and extinction. These weights are estimated from the background galaxies' magnitudes. However, the scaling of the physical cross-correlation signal with magnitude of the background galaxies is completely different. This suppression is reflected in the very low amplitude of w_cc compared to w_μ and w_τ in Fig. 3.

We assume that the optical depth of dust extinction in the lenses, τ, follows the magnification excess, $\delta\mu$, such that $\frac{2.5}{\ln(10)}\tau = c_\mathrm{d}\delta\mu$. This is motivated by the measurement by Ménard et al. (2010) with low-z galaxies but has not been shown to be true for submillimetre galaxies. We can only constrain the value of c_d at small scales where the signal-to-noise ratio is large enough to split up the LBG background sample into several magnitude bins: hence, the choice of the broad angular bin with $1.8 < \theta < 6.0$ arcsec in Fig. 2. However, our measurement over 1 deg^2 is not powerful enough to fully constrain the angular dependence of the extinction. Future measurements over larger areas could exploit the reddening effect (Ménard et al. 2010)

[6] It should be noted that the estimate from infrared abundance matching is associated with a number of systematic errors that are not present in the magnification measurement.

to constrain this dependence and potentially even the extinction law of the dust in submillimetre galaxies.

For consistency, we also calculate models where the dust is assumed to be distributed according to an exponential profile with different scale lengths $h_R = 5$–40 kpc instead of an NFW-like dust halo. The factor c_d becomes a function of angular scale then, and so do the weights for the optimally weighted correlation function. The overall amplitude of these dust models is fixed by the measured, integrated value of c_d at small scales (see Fig. 2). The best-fitting mass for such models is smaller by a factor of 2–3 than the best-fitting mass for the model with an NFW-like dust halo – the larger the scale length the smaller the discrepancy. However, the reduced χ^2 of these model fits to the data, $\chi^2/\mathrm{dof} = 2$–5, is considerably larger than the fiducial $\chi^2/\mathrm{dof} = 1.5$ of the model with an NFW-like dust component – again with the largest dust scale length (40 kpc) yielding the smallest χ^2/dof. This indicates that the dust is indeed very widely distributed, and our measurements favour the fiducial model where 'dust follows mass'. It should be stressed that we do not interpret the results in such a way that these submillimetre galaxies have a smooth NFW-like dust halo or exponential dust discs with very large scale-lengths of $h_R \gtrsim 40$ kpc. It is, however, possible that some additional, widely extended dust component – similar to what is found in Ménard et al. (2010) – is responsible for the effect seen here.

Another consequence of the limited signal-to-noise ratio is that we cannot fit a multiparameter model to the data points in Fig. 3. For this reason we concentrate on small angular scales, where a single halo can be assumed to dominate (one-halo term). The contributions from other haloes (two-halo term) only become important at larger angular scales and can be neglected here for simplicity. Further assuming a mass–concentration relation (Prada et al. 2012) for the NFW halo leaves us with just one parameter to fit, the average mass M_{200}. We check the influence of our choice of a particular mass–concentration relation by also implementing the relation by Muñoz-Cuartas et al. (2011) and find a negligible difference in the best-fitting mass of $\Delta\log_{10}[M_{200}/\mathrm{M}_\odot] \approx 0.03$. Again, the interpretation of a measurement from a more powerful, larger area survey could easily be extended to constrain the halo-occupation distributions, satellite fractions and concentration parameters directly.

We also assume that all submillimetre galaxies are central galaxies to their haloes. There are some indications in the literature from clustering studies that a fair fraction of the galaxies in such a submillimetre sample are in fact satellites (∼25 per cent for our lens sample; see Cooray et al. 2010). In the regime probed here the magnification excess, δ_μ, is fairly linear in the mass. Thus, assuming a worst-case scenario, where no mass would be associated with 25 per cent of our lenses, this would lead to an underestimate of the halo mass of the remaining 75 per cent central galaxies of $\Delta\log_{10}[M_{200}/\mathrm{M}_\odot] \approx 0.1$. This is similar to the statistical error of our measurement so that we decided not to correct for this directly here, especially because the real effect is certainly smaller than this worst-case scenario.

7 SUMMARY AND OUTLOOK

In this paper we show how to use the magnification effect of WL to measure the average mass of submillimetre galaxies. Using submillimetre galaxies as the lenses and LBGs as the sources we find a mass of $\log_{10}[M_{200}/\mathrm{M}_\odot] = 13.17^{+0.05}_{-0.08}$(stat.) for the haloes hosting the submillimetre galaxies. The presence of significant amounts of extinction by dust in the lenses complicates this measurement. However, accounting for the dust allows us to simultaneously constrain the dust mass fraction of the lenses to $M_{\mathrm{dust}}/M_{200} \approx 6 \times 10^{-5}$.

With deep, large-area imaging surveys [Dark Energy Survey (DES), Large Synoptic Survey Telescope (LSST), *Euclid*] on the horizon, WL magnification methods will gain additional importance. The higher the redshifts of the objects under study, the fewer the techniques that can provide a reliable mass measurement. As we have shown in this paper, magnification can provide such mass estimates for high-redshift objects. Follow-up observations of the optical surveys mentioned above with submillimetre telescopes will provide very large samples of high-z star-forming galaxies. Refined magnification measurements of the kind presented here, alongside with clustering measurements and other techniques, will yield unprecedented insights into the physical processes of star formation in the first half of the Universe.

Future measurements with better statistics will enable the lensing and extinction effects to be separated. Additional redshift information for the submillimetre galaxies will lead to more accurate mass estimates. By splitting the submillimetre galaxy sample in brightness it will be possible to directly study the relationship between mass and SFR.

This study shows that extinction cannot be neglected in magnification studies. The studies by Hildebrandt et al. (2009b) and Morrison et al. (2012) show excessive anticorrelations when very faint sources are used. Also the amplitudes of the angular correlation function presented there turn over from positive to negative at brighter source magnitudes than expected from magnification alone. This hints at extinction playing a role. The framework outlined here can explain this effect, and we strongly suggest future magnification studies to account for extinction to avoid a systematic bias.

ACKNOWLEDGMENTS

Herschel is an ESA space observatory with science instruments provided by European-led Principal Investigator consortia and with important participation from NASA.

SPIRE has been developed by a consortium of institutes led by Cardiff University (UK) and including Univ. Lethbridge (Canada); NAOC (China); CEA, LAM (France); IFSI, Univ. Padua (Italy); IAC (Spain); Stockholm Observatory (Sweden); Imperial College London, RAL, UCL-MSSL, UKATC, Univ. Sussex (UK) and Caltech/JPL, IPAC, Univ. Colorado (USA). This development has been supported by national funding agencies: CSA (Canada); NAOC (China); CEA, CNES, CNRS (France); ASI (Italy); MCINN (Spain); SNSB (Sweden); STFC, UKSA (UK) and NASA (USA).

This research has made use of data from the HerMES project (http://hermes.sussex.ac.uk/). HerMES is a *Herschel* Key Programme utilizing Guaranteed Time from the SPIRE instrument team, ESAC scientists and a mission scientist.

The HerMES data were accessed through the HeDaM data base (http://hedam.oamp.fr) operated by CeSAM and hosted by the Laboratoire d'Astrophysique de Marseille.

The optical data are based on observations obtained with MegaPrime/MegaCam, a joint project of CFHT and CEA/DAPNIA, at the Canada–France–Hawaii Telescope (CFHT) which is operated by the National Research Council (NRC) of Canada, the Institut National des Sciences de l'Univers of the Centre National de la Recherche Scientifique (CNRS) of France and the University of Hawaii. This work is based in part on data products produced at TERAPIX and the Canadian Astronomy Data Centre, as part of the Canada–France–Hawaii Telescope Legacy Survey, a collaborative project of NRC and CNRS.

HH is supported by the Marie Curie IOF 252760, a CITA National Fellowship and the DFG grant Hi 1495/2-1. LvW is supported by NSERC and CIfAR. DS acknowledges support by NSERC and CSA. TE is supported by the Deutsche Forschungsgemeinschaft through project ER 327/3-1 and the Transregional Collaborative Research Centre TR 33 – 'The Dark Universe'. RFJvdB acknowledges support from the Netherlands Organisation for Scientic Research grant number 639.042.814.

Author Contributions: HH led the analysis and wrote the draft version of the paper. LvW and DS contributed significantly in the development of this project through ideas and discussions on a daily basis. MB provided the redshift distribution of the submillimetre galaxies. TE led the optical data reduction and calibration. RFJvdB provided the luminosity function estimate of the background galaxies. All other co-authors contributed extensively and equally by their varied contributions to the SPIRE instrument, the Herschel mission, analysis of SPIRE and HerMES data, planning of HerMES observations and scientific support of HerMES and by commenting on this manuscript as part of an internal review process.

REFERENCES

Amblard A. et al., 2011, Nat, 470, 510
Bartelmann M., Schneider P., 2001, Phys. Rep., 340, 291
Béthermin M., Dole H., Lagache G., Le Borgne D., Penin A., 2011, A&A, 529, A4
Béthermin M., Doré O., Lagache G., 2012a, A&A, 537, L5
Béthermin M. et al., 2012b, A&A, 542, A58
Blain A. W., Longair M. S., 1993, MNRAS, 264, 509
Blake C., Pope A., Scott D., Mobasher B., 2006, MNRAS, 368, 732
Cooray A. et al., 2010, A&A, 518, L22
Eggen O. J., Lynden-Bell D., Sandage A. R., 1962, ApJ, 136, 748
Erben T. et al., 2009, A&A, 493, 1197
Faber S. M., Jackson R. E., 1976, ApJ, 204, 668
Farrah D. et al., 2006, ApJ, 641, L17
Ferrarese L., Merritt D., 2000, ApJ, 539, L9
Franceschini A., Toffolatti L., Mazzei P., Danese L., de Zotti G., 1991, A&AS, 89, 285
Griffin M. J. et al., 2010, A&A, 518, L3
Hamana T., Ouchi M., Shimasaku K., Kayo I., Suto Y., 2004, MNRAS, 347, 813
Heavens A. F., Joachimi B., 2011, MNRAS, 415, 1681
Hickox R. C. et al., 2012, MNRAS, 421, 284
Hildebrandt H., Pielorz J., Erben T., van Waerbeke L., Simon P., Capak P., 2009a, A&A, 498, 725
Hildebrandt H., van Waerbeke L., Erben T., 2009b, A&A, 507, 683
Hildebrandt H. et al., 2011, ApJ, 733, L30
Holland W. S. et al., 1999, MNRAS, 303, 659
Ivison R. J. et al., 2007, MNRAS, 380, 199
Kennicutt R. C. Jr, 1998, ApJ, 498, 541
Komatsu E. et al., 2011, ApJS, 192, 18
Landy S. D., Szalay A. S., 1993, ApJ, 412, 64
Leauthaud A. et al., 2012, ApJ, 744, 159
Limber D. N., 1953, ApJ, 117, 134
Madau P., Ferguson H. C., Dickinson M. E., Giavalisco M., Steidel C. C., Fruchter A., 1996, MNRAS, 283, 1388
Ménard B., Hamana T., Bartelmann M., Yoshida N., 2003, A&A, 403, 817
Ménard B., Scranton R., Fukugita M., Richards G., 2010, MNRAS, 405, 1025
Morrison C. B., Scranton R., Ménard B., Schmidt S. J., Tyson J. A., Ryan R., Choi A., Wittman D. M., 2012, MNRAS, 426, 2489
Muñoz-Cuartas J. C., Macciò A. V., Gottlöber S., Dutton A. A., 2011, MNRAS, 411, 584
Navarro J. F., Frenk C. S., White S. D. M., 1996, ApJ, 462, 563
Oliver S. J. et al., 2010, A&A, 518, L21
Oliver S. J. et al., 2012, MNRAS, 424, 1614
Pilbratt G. L. et al., 2010, A&A, 518, L1
Prada F., Klypin A. A., Cuesta A. J., Betancort-Rijo J. E., Primack J., 2012, MNRAS, 423, 3018
Roseboom I. G. et al., 2010, MNRAS, 409, 48
Scoville N. et al., 2007, ApJS, 172, 1
Scranton R. et al., 2005, ApJ, 633, 589
Steidel C. C., Giavalisco M., Pettini M., Dickinson M., Adelberger K. L., 1996, ApJ, 462, L17
Tully R. B., Fisher J. R., 1977, A&A, 54, 661
van der Burg R. F. J., Hildebrandt H., Erben T., 2010, A&A, 523, A74
van Waerbeke L., Hildebrandt H., Ford J., Milkeraitis M., 2010, ApJ, 723, L13
Viero M. P. et al., 2012, preprint (arXiv:1008.4359)
Wang L. et al., 2011, MNRAS, 414, 596
Wright C. O., Brainerd T. G., 2000, ApJ, 534, 34

This paper has been typeset from a TEX/LATEX file prepared by the author.